

Measurement of W -Boson Polarization in Top-quark Decay in $p\bar{p}$ Collisions at $\sqrt{s} = 1.96$ TeV

T. Aaltonen,²⁴ J. Adelman,¹⁴ B. Álvarez González^{w,12} S. Amerio^{ee,44} D. Amidei,³⁵ A. Anastassov,³⁹ A. Annovi,²⁰ J. Antos,¹⁵ G. Apollinari,¹⁸ J. Appel,¹⁸ A. Apresyan,⁴⁹ T. Arisawa,⁵⁸ A. Artikov,¹⁶ J. Asaadi,⁵⁴ W. Ashmanskas,¹⁸ A. Attal,⁴ A. Aurisano,⁵⁴ F. Azfar,⁴³ W. Badgett,¹⁸ A. Barbaro-Galtieri,²⁹ V.E. Barnes,⁴⁹ B.A. Barnett,²⁶ P. Barria^{gg,47} P. Bartos,¹⁵ G. Bauer,³³ P.-H. Beauchemin,³⁴ F. Bedeschi,⁴⁷ D. Beecher,³¹ S. Behari,²⁶ G. Bellettini^{ff,47} J. Bellinger,⁶⁰ D. Benjamin,¹⁷ A. Beretvas,¹⁸ A. Bhatti,⁵¹ M. Binkley*,¹⁸ D. Bisello^{ee,44} I. Bizjak^{kk,31} R.E. Blair,² C. Blocker,⁷ B. Blumenfeld,²⁶ A. Bocci,¹⁷ A. Bodek,⁵⁰ V. Boisvert,⁵⁰ D. Bortoletto,⁴⁹ J. Boudreau,⁴⁸ A. Boveia,¹¹ B. Brau^{a,11} A. Bridgeman,²⁵ L. Brigliadori^{dd,6} C. Bromberg,³⁶ E. Brubaker,¹⁴ J. Budagov,¹⁶ H.S. Budd,⁵⁰ S. Budd,²⁵ K. Burkett,¹⁸ G. Busetto^{ee,44} P. Bussey,²² A. Buzatu,³⁴ K. L. Byrum,² S. Cabrera^{y,17} C. Calancha,³² S. Camarda,⁴ M. Campanelli,³¹ M. Campbell,³⁵ F. Canelli^{14,18} A. Canepa,⁴⁶ B. Carls,²⁵ D. Carlsmith,⁶⁰ R. Carosi,⁴⁷ S. Carrillo^{n,19} S. Carron,¹⁸ B. Casal,¹² M. Casarsa,¹⁸ A. Castro^{dd,6} P. Catastini^{gg,47} D. Cauz,⁵⁵ V. Cavaliere^{gg,47} M. Cavalli-Sforza,⁴ A. Cerri,²⁹ L. Cerrito^{q,31} S.H. Chang,²⁸ Y.C. Chen,¹ M. Chertok,⁸ G. Chiarelli,⁴⁷ G. Chlachidze,¹⁸ F. Chlebana,¹⁸ K. Cho,²⁸ D. Chokheli,¹⁶ J.P. Chou,²³ K. Chung^{o,18} W.H. Chung,⁶⁰ Y.S. Chung,⁵⁰ T. Chwalek,²⁷ C.I. Ciobanu,⁴⁵ M.A. Ciocci^{gg,47} A. Clark,²¹ D. Clark,⁷ G. Compostella,⁴⁴ M.E. Convery,¹⁸ J. Conway,⁸ M. Corbo,⁴⁵ M. Cordelli,²⁰ C.A. Cox,⁸ D.J. Cox,⁸ F. Crescioli^{ff,47} C. Cuenca Almenar,⁶¹ J. Cuevas^{w,12} R. Culbertson,¹⁸ J.C. Cully,³⁵ D. Dagenhart,¹⁸ N. d'Ascenzo^{v,45} M. Datta,¹⁸ T. Davies,²² P. de Barbaro,⁵⁰ S. De Cecco,⁵² A. Deisher,²⁹ G. De Lorenzo,⁴ M. Dell'Orso^{ff,47} C. Deluca,⁴ L. Demortier,⁵¹ J. Deng^{f,17} M. Deninno,⁶ M. d'Errico^{ee,44} A. Di Canto^{ff,47} B. Di Ruzza,⁴⁷ J.R. Dittmann,⁵ M. D'Onofrio,⁴ S. Donati^{ff,47} P. Dong,¹⁸ T. Dorigo,⁴⁴ S. Dube,⁵³ K. Ebina,⁵⁸ A. Elagin,⁵⁴ R. Erbacher,⁸ D. Errede,²⁵ S. Errede,²⁵ N. Ershaidat^{cc,45} R. Eusebi,⁵⁴ H.C. Fang,²⁹ S. Farrington,⁴³ W.T. Fedorko,¹⁴ R.G. Feild,⁶¹ M. Feindt,²⁷ J.P. Fernandez,³² C. Ferrazza^{hh,47} R. Field,¹⁹ G. Flanagan^{s,49} R. Forrest,⁸ M.J. Frank,⁵ M. Franklin,²³ J.C. Freeman,¹⁸ I. Furic,¹⁹ M. Gallinaro,⁵¹ J. Galyardt,¹³ F. Garbersen,¹¹ J.E. Garcia,²¹ A.F. Garfinkel,⁴⁹ P. Garosi^{gg,47} H. Gerberich,²⁵ D. Gerdes,³⁵ A. Gessler,²⁷ S. Giagu^{ii,52} V. Giakoumopoulou,³ P. Giannetti,⁴⁷ K. Gibson,⁴⁸ J.L. Gimmell,⁵⁰ C.M. Ginsburg,¹⁸ N. Giokaris,³ M. Giordani^{jj,55} P. Giromini,²⁰ M. Giunta,⁴⁷ G. Giurgiu,²⁶ V. Glagolev,¹⁶ D. Glenzinski,¹⁸ M. Gold,³⁸ N. Goldschmidt,¹⁹ A. Golossanov,¹⁸ G. Gomez,¹² G. Gomez-Ceballos,³³ M. Goncharov,³³ O. González,³² I. Gorelov,³⁸ A.T. Goshaw,¹⁷ K. Goulianos,⁵¹ A. Gresele^{ee,44} S. Grinstein,⁴ C. Grosso-Pilcher,¹⁴ R.C. Group,¹⁸ U. Grundler,²⁵ J. Guimaraes da Costa,²³ Z. Gunay-Unalan,³⁶ C. Haber,²⁹ S.R. Hahn,¹⁸ E. Halkiadakis,⁵³ B.-Y. Han,⁵⁰ J.Y. Han,⁵⁰ F. Happacher,²⁰ K. Hara,⁵⁶ D. Hare,⁵³ M. Hare,⁵⁷ R.F. Harr,⁵⁹ M. Hartz,⁴⁸ K. Hatakeyama,⁵ C. Hays,⁴³ M. Heck,²⁷ J. Heinrich,⁴⁶ M. Herndon,⁶⁰ J. Heuser,²⁷ S. Hewamanage,⁵ D. Hidas,⁵³ C.S. Hill^{c,11} D. Hirschbuehl,²⁷ A. Hocker,¹⁸ S. Hou,¹ M. Houlden,³⁰ S.-C. Hsu,²⁹ R.E. Hughes,⁴⁰ M. Hurwitz,¹⁴ U. Husemann,⁶¹ M. Hussein,³⁶ J. Huston,³⁶ J. Incandela,¹¹ G. Introzzi,⁴⁷ M. Iori^{ii,52} A. Ivanov^{p,8} E. James,¹⁸ D. Jang,¹³ B. Jayatilaka,¹⁷ E.J. Jeon,²⁸ M.K. Jha,⁶ S. Jindariani,¹⁸ W. Johnson,⁸ M. Jones,⁴⁹ K.K. Joo,²⁸ S.Y. Jun,¹³ J.E. Jung,²⁸ T.R. Junk,¹⁸ T. Kamon,⁵⁴ D. Kar,¹⁹ P.E. Karchin,⁵⁹ Y. Kato^{m,42} R. Kephart,¹⁸ W. Ketchum,¹⁴ J. Keung,⁴⁶ V. Khotilovich,⁵⁴ B. Kilminster,¹⁸ D.H. Kim,²⁸ H.S. Kim,²⁸ H.W. Kim,²⁸ J.E. Kim,²⁸ M.J. Kim,²⁰ S.B. Kim,²⁸ S.H. Kim,⁵⁶ Y.K. Kim,¹⁴ N. Kimura,⁵⁸ L. Kirsch,⁷ S. Klimenko,¹⁹ K. Kondo,⁵⁸ D.J. Kong,²⁸ J. Konigsberg,¹⁹ A. Korytov,¹⁹ A.V. Kotwal,¹⁷ M. Kreps,²⁷ J. Kroll,⁴⁶ D. Krop,¹⁴ N. Krumnack,⁵ M. Kruse,¹⁷ V. Krutelyov,¹¹ T. Kuhr,²⁷ N.P. Kulkarni,⁵⁹ M. Kurata,⁵⁶ S. Kwang,¹⁴ A.T. Laasanen,⁴⁹ S. Lami,⁴⁷ S. Lammel,¹⁸ M. Lancaster,³¹ R.L. Lander,⁸ K. Lannon^{u,40} A. Lath,⁵³ G. Latino^{gg,47} I. Lazzizzera^{ee,44} T. LeCompte,² E. Lee,⁵⁴ H.S. Lee,¹⁴ J.S. Lee,²⁸ S.W. Lee^{x,54} S. Leone,⁴⁷ J.D. Lewis,¹⁸ C.-J. Lin,²⁹ J. Linacre,⁴³ M. Lindgren,¹⁸ E. Lipeles,⁴⁶ A. Lister,²¹ D.O. Litvintsev,¹⁸ C. Liu,⁴⁸ T. Liu,¹⁸ N.S. Lockyer,⁴⁶ A. Loginov,⁶¹ L. Lovas,¹⁵ D. Lucchesi^{ee,44} J. Lueck,²⁷ P. Lujan,²⁹ P. Lukens,¹⁸ G. Lungu,⁵¹ J. Lys,²⁹ R. Lysak,¹⁵ D. MacQueen,³⁴ R. Madrak,¹⁸ K. Maeshima,¹⁸ K. Makhoul,³³ P. Maksimovic,²⁶ S. Malde,⁴³ S. Malik,³¹ G. Manca^{e,30} A. Manousakis-Katsikakis,³ F. Margaroli,⁴⁹ C. Marino,²⁷ C.P. Marino,²⁵ A. Martin,⁶¹ V. Martin^{k,22} M. Martínez,⁴ R. Martínez-Ballarín,³² P. Mastrandrea,⁵² M. Mathis,²⁶ M.E. Mattson,⁵⁹ P. Mazzanti,⁶ K.S. McFarland,⁵⁰ P. McIntyre,⁵⁴ R. McNulty^{j,30} A. Mehta,³⁰ P. Mehtala,²⁴ A. Menzione,⁴⁷ C. Mesropian,⁵¹ T. Miao,¹⁸ D. Mietlicki,³⁵ N. Miladinovic,⁷ R. Miller,³⁶ C. Mills,²³ M. Milnik,²⁷ A. Mitra,¹ G. Mitselmakher,¹⁹ H. Miyake,⁵⁶ S. Moed,²³ N. Moggi,⁶ M.N. Mondragon^{n,18} C.S. Moon,²⁸ R. Moore,¹⁸ M.J. Morello,⁴⁷ J. Morlock,²⁷ P. Movilla Fernandez,¹⁸ J. Müllenstädt,²⁹ A. Mukherjee,¹⁸ Th. Muller,²⁷ P. Murat,¹⁸ M. Mussini^{dd,6} J. Nachtman^{o,18} Y. Nagai,⁵⁶ J. Naganoma,⁵⁶ K. Nakamura,⁵⁶ I. Nakano,⁴¹ A. Napier,⁵⁷ J. Nett,⁶⁰ C. Neu^{aa,46}

M.S. Neubauer,²⁵ S. Neubauer,²⁷ J. Nielsen^g,²⁹ L. Nodulman,² M. Norman,¹⁰ O. Norniella,²⁵ E. Nurse,³¹ L. Oakes,⁴³ S.H. Oh,¹⁷ Y.D. Oh,²⁸ I. Oksuzian,¹⁹ T. Okusawa,⁴² R. Orava,²⁴ K. Osterberg,²⁴ S. Pagan Griso^{ee},⁴⁴ C. Pagliarone,⁵⁵ E. Palencia,¹⁸ V. Papadimitriou,¹⁸ A. Papaikonomou,²⁷ A.A. Paramanov,² B. Parks,⁴⁰ S. Pashapour,³⁴ J. Patrick,¹⁸ G. Pauletta^{jj},⁵⁵ M. Paulini,¹³ C. Paus,³³ T. Peiffer,²⁷ D.E. Pellett,⁸ A. Penzo,⁵⁵ T.J. Phillips,¹⁷ G. Piacentino,⁴⁷ E. Pianori,⁴⁶ L. Pinera,¹⁹ K. Pitts,²⁵ C. Plager,⁹ L. Pondrom,⁶⁰ K. Potamianos,⁴⁹ O. Poukhov^{*},¹⁶ F. Prokoshin^z,¹⁶ A. Pronko,¹⁸ F. Ptohosⁱ,¹⁸ E. Pueschel,¹³ G. Punzi^{ff},⁴⁷ J. Pursley,⁶⁰ J. Rademacker^c,⁴³ A. Rahaman,⁴⁸ V. Ramakrishnan,⁶⁰ N. Ranjan,⁴⁹ I. Redondo,³² P. Renton,⁴³ M. Renz,²⁷ M. Rescigno,⁵² S. Richter,²⁷ F. Rimondi^{dd},⁶ L. Ristori,⁴⁷ A. Robson,²² T. Rodrigo,¹² T. Rodriguez,⁴⁶ E. Rogers,²⁵ S. Rolli,⁵⁷ R. Roser,¹⁸ M. Rossi,⁵⁵ R. Rossin,¹¹ P. Roy,³⁴ A. Ruiz,¹² J. Russ,¹³ V. Rusu,¹⁸ B. Rutherford,¹⁸ H. Saarikko,²⁴ A. Safonov,⁵⁴ W.K. Sakumoto,⁵⁰ L. Santi^{jj},⁵⁵ L. Sartori,⁴⁷ K. Sato,⁵⁶ V. Saveliev^v,⁴⁵ A. Savoy-Navarro,⁴⁵ P. Schlabach,¹⁸ A. Schmidt,²⁷ E.E. Schmidt,¹⁸ M.A. Schmidt,¹⁴ M.P. Schmidt^{*},⁶¹ M. Schmitt,³⁹ T. Schwarz,⁸ L. Scodellaro,¹² A. Scribano^{gg},⁴⁷ F. Scuri,⁴⁷ A. Sedov,⁴⁹ S. Seidel,³⁸ Y. Seiya,⁴² A. Semenov,¹⁶ L. Sexton-Kennedy,¹⁸ F. Sforza^{ff},⁴⁷ A. Sfyrila,²⁵ S.Z. Shalhout,⁵⁹ T. Shears,³⁰ P.F. Shepard,⁴⁸ M. Shimojima^t,⁵⁶ S. Shiraishi,¹⁴ M. Shochet,¹⁴ Y. Shon,⁶⁰ I. Shreyber,³⁷ A. Simonenko,¹⁶ P. Sinervo,³⁴ A. Sisakyan,¹⁶ A.J. Slaughter,¹⁸ J. Slaunwhite,⁴⁰ K. Sliwa,⁵⁷ J.R. Smith,⁸ F.D. Snider,¹⁸ R. Snihur,³⁴ A. Soha,¹⁸ S. Somalwar,⁵³ V. Sorin,⁴ P. Squillacioti^{gg},⁴⁷ M. Stanitzki,⁶¹ R. St. Denis,²² B. Stelzer,³⁴ O. Stelzer-Chilton,³⁴ D. Stentz,³⁹ J. Strogas,³⁸ G.L. Strycker,³⁵ J.S. Suh,²⁸ A. Sukhanov,¹⁹ I. Suslov,¹⁶ A. Taffard^f,²⁵ R. Takashima,⁴¹ Y. Takeuchi,⁵⁶ R. Tanaka,⁴¹ J. Tang,¹⁴ M. Tecchio,³⁵ P.K. Teng,¹ J. Thom^h,¹⁸ J. Thome,¹³ G.A. Thompson,²⁵ E. Thomson,⁴⁶ P. Tipton,⁶¹ P. Ttito-Guzmán,³² S. Tkaczyk,¹⁸ D. Toback,⁵⁴ S. Tokar,¹⁵ K. Tollefson,³⁶ T. Tomura,⁵⁶ D. Tonelli,¹⁸ S. Torre,²⁰ D. Torretta,¹⁸ P. Totaro^{jj},⁵⁵ M. Trovato^{hh},⁴⁷ S.-Y. Tsai,¹ Y. Tu,⁴⁶ N. Turini^{gg},⁴⁷ F. Ukegawa,⁵⁶ S. Uozumi,²⁸ N. van Remortel^b,²⁴ A. Varganov,³⁵ E. Vataga^{hh},⁴⁷ F. Vázquezⁿ,¹⁹ G. Velev,¹⁸ C. Vellidis,³ M. Vidal,³² I. Vila,¹² R. Vilar,¹² M. Vogel,³⁸ I. Volobouev^x,²⁹ G. Volpi^{ff},⁴⁷ P. Wagner,⁴⁶ R.G. Wagner,² R.L. Wagner,¹⁸ W. Wagner^{bb},²⁷ J. Wagner-Kuhr,²⁷ T. Wakisaka,⁴² R. Wallny,⁹ S.M. Wang,¹ A. Warburton,³⁴ D. Waters,³¹ M. Weinberger,⁵⁴ J. Weinel,²⁷ W.C. Wester III,¹⁸ B. Whitehouse,⁵⁷ D. Whiteson^f,⁴⁶ A.B. Wicklund,² E. Wicklund,¹⁸ S. Wilbur,¹⁴ G. Williams,³⁴ H.H. Williams,⁴⁶ P. Wilson,¹⁸ B.L. Winer,⁴⁰ P. Wittich^h,¹⁸ S. Wolbers,¹⁸ C. Wolfe,¹⁴ H. Wolfe,⁴⁰ T. Wright,³⁵ X. Wu,²¹ F. Würthwein,¹⁰ A. Yagil,¹⁰ K. Yamamoto,⁴² J. Yamaoka,¹⁷ U.K. Yang^r,¹⁴ Y.C. Yang,²⁸ W.M. Yao,²⁹ G.P. Yeh,¹⁸ K. Yi^o,¹⁸ J. Yoh,¹⁸ K. Yorita,⁵⁸ T. Yoshida^l,⁴² G.B. Yu,¹⁷ I. Yu,²⁸ S.S. Yu,¹⁸ J.C. Yun,¹⁸ A. Zanetti,⁵⁵ Y. Zeng,¹⁷ X. Zhang,²⁵ Y. Zheng^d,⁹ and S. Zucchelli^{dd6}

(CDF Collaboration[†])

¹*Institute of Physics, Academia Sinica, Taipei, Taiwan 11529, Republic of China*

²*Argonne National Laboratory, Argonne, Illinois 60439, USA*

³*University of Athens, 157 71 Athens, Greece*

⁴*Institut de Fisica d'Altes Energies, Universitat Autònoma de Barcelona, E-08193, Bellaterra (Barcelona), Spain*

⁵*Baylor University, Waco, Texas 76798, USA*

⁶*Istituto Nazionale di Fisica Nucleare Bologna, ^{dd}University of Bologna, I-40127 Bologna, Italy*

⁷*Brandeis University, Waltham, Massachusetts 02254, USA*

⁸*University of California, Davis, Davis, California 95616, USA*

⁹*University of California, Los Angeles, Los Angeles, California 90024, USA*

¹⁰*University of California, San Diego, La Jolla, California 92093, USA*

¹¹*University of California, Santa Barbara, Santa Barbara, California 93106, USA*

¹²*Instituto de Fisica de Cantabria, CSIC-University of Cantabria, 39005 Santander, Spain*

¹³*Carnegie Mellon University, Pittsburgh, Pennsylvania 15213, USA*

¹⁴*Enrico Fermi Institute, University of Chicago, Chicago, Illinois 60637, USA*

¹⁵*Comenius University, 842 48 Bratislava, Slovakia; Institute of Experimental Physics, 040 01 Kosice, Slovakia*

¹⁶*Joint Institute for Nuclear Research, RU-141980 Dubna, Russia*

¹⁷*Duke University, Durham, North Carolina 27708, USA*

¹⁸*Fermi National Accelerator Laboratory, Batavia, Illinois 60510, USA*

¹⁹*University of Florida, Gainesville, Florida 32611, USA*

²⁰*Laboratori Nazionali di Frascati, Istituto Nazionale di Fisica Nucleare, I-00044 Frascati, Italy*

²¹*University of Geneva, CH-1211 Geneva 4, Switzerland*

²²*Glasgow University, Glasgow G12 8QQ, United Kingdom*

²³*Harvard University, Cambridge, Massachusetts 02138, USA*

²⁴*Division of High Energy Physics, Department of Physics,*

University of Helsinki and Helsinki Institute of Physics, FIN-00014, Helsinki, Finland

²⁵*University of Illinois, Urbana, Illinois 61801, USA*

²⁶*The Johns Hopkins University, Baltimore, Maryland 21218, USA*

- ²⁷*Institut für Experimentelle Kernphysik, Karlsruhe Institute of Technology, D-76131 Karlsruhe, Germany*
- ²⁸*Center for High Energy Physics: Kyungpook National University, Daegu 702-701, Korea; Seoul National University, Seoul 151-742, Korea; Sungkyunkwan University, Suwon 440-746, Korea; Korea Institute of Science and Technology Information, Daejeon 305-806, Korea; Chonnam National University, Gwangju 500-757, Korea; Chonbuk National University, Jeonju 561-756, Korea*
- ²⁹*Ernest Orlando Lawrence Berkeley National Laboratory, Berkeley, California 94720, USA*
- ³⁰*University of Liverpool, Liverpool L69 7ZE, United Kingdom*
- ³¹*University College London, London WC1E 6BT, United Kingdom*
- ³²*Centro de Investigaciones Energeticas Medioambientales y Tecnologicas, E-28040 Madrid, Spain*
- ³³*Massachusetts Institute of Technology, Cambridge, Massachusetts 02139, USA*
- ³⁴*Institute of Particle Physics: McGill University, Montréal, Québec, Canada H3A 2T8; Simon Fraser University, Burnaby, British Columbia, Canada V5A 1S6; University of Toronto, Toronto, Ontario, Canada M5S 1A7; and TRIUMF, Vancouver, British Columbia, Canada V6T 2A3*
- ³⁵*University of Michigan, Ann Arbor, Michigan 48109, USA*
- ³⁶*Michigan State University, East Lansing, Michigan 48824, USA*
- ³⁷*Institution for Theoretical and Experimental Physics, ITEP, Moscow 117259, Russia*
- ³⁸*University of New Mexico, Albuquerque, New Mexico 87131, USA*
- ³⁹*Northwestern University, Evanston, Illinois 60208, USA*
- ⁴⁰*The Ohio State University, Columbus, Ohio 43210, USA*
- ⁴¹*Okayama University, Okayama 700-8530, Japan*
- ⁴²*Osaka City University, Osaka 588, Japan*
- ⁴³*University of Oxford, Oxford OX1 3RH, United Kingdom*
- ⁴⁴*Istituto Nazionale di Fisica Nucleare, Sezione di Padova-Trento, ^{ee} University of Padova, I-35131 Padova, Italy*
- ⁴⁵*LPNHE, Universite Pierre et Marie Curie/IN2P3-CNRS, UMR7585, Paris, F-75252 France*
- ⁴⁶*University of Pennsylvania, Philadelphia, Pennsylvania 19104, USA*
- ⁴⁷*Istituto Nazionale di Fisica Nucleare Pisa, ^{ff} University of Pisa, ^{gg} Scuola Normale Superiore, I-56127 Pisa, Italy*
- ⁴⁸*University of Pittsburgh, Pittsburgh, Pennsylvania 15260, USA*
- ⁴⁹*Purdue University, West Lafayette, Indiana 47907, USA*
- ⁵⁰*University of Rochester, Rochester, New York 14627, USA*
- ⁵¹*The Rockefeller University, New York, New York 10021, USA*
- ⁵²*Istituto Nazionale di Fisica Nucleare, Sezione di Roma 1, ⁱⁱ Sapienza Università di Roma, I-00185 Roma, Italy*
- ⁵³*Rutgers University, Piscataway, New Jersey 08855, USA*
- ⁵⁴*Texas A&M University, College Station, Texas 77843, USA*
- ⁵⁵*Istituto Nazionale di Fisica Nucleare Trieste/Udine, I-34100 Trieste, ^{jj} University of Trieste/Udine, I-33100 Udine, Italy*
- ⁵⁶*University of Tsukuba, Tsukuba, Ibaraki 305, Japan*
- ⁵⁷*Tufts University, Medford, Massachusetts 02155, USA*
- ⁵⁸*Waseda University, Tokyo 169, Japan*
- ⁵⁹*Wayne State University, Detroit, Michigan 48201, USA*
- ⁶⁰*University of Wisconsin, Madison, Wisconsin 53706, USA*
- ⁶¹*Yale University, New Haven, Connecticut 06520, USA*
- (Dated: June 6, 2018)

We report measurements of the polarization of W bosons from top-quark decays using 2.7 fb^{-1} of $p\bar{p}$ collisions collected by the CDF II detector. Assuming a top-quark mass of $175 \text{ GeV}/c^2$, three measurements are performed. A simultaneous measurement of the fraction of longitudinal (f_0) and right-handed (f_+) W bosons yields the model-independent results $f_0 = 0.88 \pm 0.11(\text{stat}) \pm 0.06(\text{syst})$ and $f_+ = -0.15 \pm 0.07(\text{stat}) \pm 0.06(\text{syst})$ with a correlation coefficient of -0.59 . A measurement of f_0 (f_+) constraining f_+ (f_0) to its standard model value of 0.0 (0.7) yields $f_0 = 0.70 \pm 0.07(\text{stat}) \pm 0.04(\text{syst})$ ($f_+ = -0.01 \pm 0.02(\text{stat}) \pm 0.05(\text{syst})$). All these results are consistent with standard model expectations.

PACS numbers: 14.65.Ha, 14.80.Cp, 13.85.Ni, 13.85.Qk, 14.70.Dj

*Deceased

†With visitors from ^{aa}University of Massachusetts Amherst,

The top quark is the most massive fundamental particle observed by experiment [1]. Due to its large mass, in the standard model (SM) the top quark decays before forming a bound state via the charged current weak interaction into a W^+ boson and a b quark [2], with a branching fraction above 99% [3]. This provides a unique opportunity to study the properties of a “bare” quark. In particular, the $V - A$ structure of the weak interaction can be tested by reconstructing the polarization of the W^+ boson from top-quark decay. In the standard model (SM) at tree level [4], the W^+ boson is expected to have longitudinal polarization $f_0 = 0.703$, left-handed polarization $f_- = 0.297$, and right-handed polarization $f_+ = 3.6 \times 10^{-4}$ for a top-quark mass $m_t = 175 \text{ GeV}/c^2$, a W -boson mass $M_W = 80.413 \text{ GeV}/c^2$ [5], and a b -quark mass $m_b = 4.79 \text{ GeV}/c^2$ [3]. In the limit of $m_b \rightarrow 0$, $f_0 = m_t^2/(2m_W^2 + m_t^2)$ and $f_+ = 0$. The higher-order QCD and electroweak radiative corrections modify these predictions at the 1-2% (relative) level [6]. In beyond-the-SM scenarios, significant deviations from the SM expectation are possible due to the presence of anomalous couplings [4] in the tWb vertex. Measurements of W -boson polarization and single top-quark production together set constraints on the anomalous coupling vector and tensor form factors [7].

In this Letter, we measure the polarization of the W boson from top-quark decay. We assume the $t\bar{t}$ production mechanism is in agreement with the SM, and we study a data sample enriched in $t\bar{t} \rightarrow W^+bW^-\bar{b} \rightarrow \ell\nu b\bar{q}\bar{q}'\bar{b}$ events where one of the W bosons decays hadronically and the other leptonically. We apply a likeli-

hood technique based on the theoretical matrix elements for both the dominant signal process, $q\bar{q} \rightarrow t\bar{t}$, and the main background process, inclusive production of W +jets. This technique was first developed for the measurements of top-quark mass and f_0 , constraining f_+ to its SM value [8], and utilizes the kinematic and topological information from the event through integrations over poorly known parton-level quantities. We express the matrix element in terms of the W -boson polarization fractions and the cosine of the angle θ^* between the momentum of the charged lepton or down-type quark in the W -boson rest frame and the momentum of the W boson in the top-quark rest frame. Therefore we extract information on the W -boson polarization from both the leptonic and hadronic W -boson decays. Previous CDF measurements [9, 10] used only information from the leptonic decay via the transverse momentum p_T [11] of the lepton, $\cos\theta^*$ for the leptonically decaying W boson, or the invariant mass of each lepton and b -jet pair, which is a function of $\cos\theta^*$. While the information from the hadronic W -boson decay carries a sign ambiguity in $\cos\theta^*$ since we are unable to identify the down-type quark jet its inclusion still improves the sensitivity to the f_0 polarization fraction. The analysis described in this letter improves the statistical sensitivity on f_0 by 20% relative to the best previous CDF measurement [9] for the same event sample. The latest D0 measurement also utilizes information from both the leptonic and hadronic W -boson decays using a likelihood fit to the $\cos\theta^*$ distributions [12].

We report measurements of the W -boson polarization for three different hypotheses of top-quark decay: (1) model-independent with simultaneous measurement of f_0 and f_+ ; (2) anomalous tensor couplings with measurement of f_0 for fixed $f_+=0$; and (3) anomalous right-handed couplings with measurement of f_+ for fixed $f_0 = 0.70$.

The polarization fractions are determined by maximizing the likelihood L with respect to f_0 , f_+ , and the fraction of events consistent with the $t\bar{t}$ signal hypothesis, C_s ,

$$L(f_0, f_+, C_s) = \prod_{i=1}^N C_s \frac{P_s(x; f_0, f_+)}{\langle A_s(x; f_0, f_+) \rangle} + (1 - C_s) \frac{P_b(x)}{\langle A_b(x) \rangle}.$$

Here N is the number of observed events, and $\langle A_s \rangle$ and $\langle A_b \rangle$ refer to the average acceptances for $t\bar{t}$ and W +jets background events, respectively. The dependence of the signal acceptance on the polarization fractions is included in $\langle A_s \rangle$. The signal probability P_s and background probability P_b densities are constructed as in [13] by integrating over the appropriate parton-level differential cross section, $d\sigma(y)/dy$, convolved with proton parton distribution functions ($f(q_1)$ and $f(q_2)$) and detector resolution effects relating a set of observed variables x to cor-

Amherst, Massachusetts 01003, ^bUniversiteit Antwerpen, B-2610 Antwerp, Belgium, ^cUniversity of Bristol, Bristol BS8 1TL, United Kingdom, ^dChinese Academy of Sciences, Beijing 100864, China, ^eIstituto Nazionale di Fisica Nucleare, Sezione di Cagliari, 09042 Monserrato (Cagliari), Italy, ^fUniversity of California Irvine, Irvine, CA 92697, ^gUniversity of California Santa Cruz, Santa Cruz, CA 95064, ^hCornell University, Ithaca, NY 14853, ⁱUniversity of Cyprus, Nicosia CY-1678, Cyprus, ^jUniversity College Dublin, Dublin 4, Ireland, ^kUniversity of Edinburgh, Edinburgh EH9 3JZ, United Kingdom, ^lUniversity of Fukui, Fukui City, Fukui Prefecture, Japan 910-0017, ^mKinki University, Higashi-Osaka City, Japan 577-8502, ⁿUniversidad Iberoamericana, Mexico D.F., Mexico, ^oUniversity of Iowa, Iowa City, IA 52242, ^pKansas State University, Manhattan, KS 66506, ^qQueen Mary, University of London, London, E1 4NS, England, ^rUniversity of Manchester, Manchester M13 9PL, England, ^sMuons, Inc., Batavia, IL 60510, ^tNagasaki Institute of Applied Science, Nagasaki, Japan, ^uUniversity of Notre Dame, Notre Dame, IN 46556, ^vObninsk State University, Obninsk, Russia, ^wUniversity de Oviedo, E-33007 Oviedo, Spain, ^xTexas Tech University, Lubbock, TX 79609, ^yIFIC(CSIC-Universitat de Valencia), 56071 Valencia, Spain, ^zUniversidad Tecnica Federico Santa Maria, 110v Valparaiso, Chile, ^{aa}University of Virginia, Charlottesville, VA 22906, ^{bb}Bergische Universität Wuppertal, 42097 Wuppertal, Germany, ^{cc}Yarmouk University, Irbid 211-63, Jordan, ^{kk}On leave from J. Stefan Institute, Ljubljana, Slovenia,

responding parton-level quantities y , $W(x, y)$:

$$P(x) = \sum_{perm.} \int \frac{d\sigma(y)}{dy} f(q_1) f(q_2) dq_1 dq_2 W(x, y) dy.$$

Here partons are identified with the four highest transverse energy E_T [11] jets, and all the corresponding jet-parton permutations are considered.

The signal differential cross section uses the leading-order matrix element of the $q\bar{q} \rightarrow t\bar{t}$ process [14], expressed in terms of $\cos\theta^*$ and polarization fractions:

$$|M|^2 = \frac{g_s^4}{9} F_{lep} \bar{F}_{had} (2 - \beta^2 \sin^2 \theta_{qt}),$$

where g_s is the strong coupling constant and θ_{qt} describes the angle between the incoming parton and the top quark in the rest frame of the incoming partons, and β is the speed of the top quarks in the same rest frame. The factors F_{lep} and \bar{F}_{had} correspond to the top quarks with a leptonic and a hadronic W -boson decay, such that:

$$F_{lep} = \frac{2\pi g_W^4 m_{\bar{\ell}\nu}^2}{3 m_t \Gamma_t} (2E_b^{*2} + 3E_b^* m_{\bar{\ell}\nu} + m_b^2) \\ (f_+ \cdot \frac{3}{8} (1 + \cos\theta^*)^2 + f_0 \cdot \frac{3}{4} (1 - \cos^2\theta^*) \\ + (1 - f_0 - f_+) \cdot \frac{3}{8} (1 - \cos\theta^*)^2).$$

Here g_W is the weak coupling constant, $m_{\bar{\ell}\nu}$ is the invariant mass of the lepton and neutrino, Γ_t is the width of the top quark, m_t and m_b are the masses of the top quark and b quark, respectively, and $E_b^* = \frac{m_t^2 - m_b^2 - m_{\bar{\ell}\nu}^2}{2m_{\bar{\ell}\nu}}$. The hadronic factor \bar{F}_{had} is similar, with the exception that we do not distinguish between up-type and down-type quarks from W -boson decay and use the average \bar{F}_{had} related to the two permutations. The background differential cross section uses the sum of matrix elements for W +jets from the VECBOS [15] Monte Carlo (MC) generator.

The measurement is based on a data set with an integrated luminosity of approximately 2.7 fb^{-1} acquired by the Collider Detector at Fermilab (CDF II) [16] from $p\bar{p}$ collisions at $\sqrt{s} = 1.96 \text{ TeV}$. The data used are collected using high- p_T central (pseudorapidity [11] $|\eta| < 1.1$) electron and muon triggers, a high- p_T forward ($1.2 < |\eta| < 2.0$) electron trigger, and a trigger that requires large missing transverse energy \cancel{E}_T [11] with either an energetic electromagnetic cluster or two separated jets (\cancel{E}_T +jets) [17]. The \cancel{E}_T +jets trigger is used to select additional events with high- p_T muons, which are not selected by the lepton triggers.

Candidate events for the lepton plus jets final state

($t\bar{t} \rightarrow W^+ b W^- \bar{b} \rightarrow \ell \nu b q \bar{q}' \bar{b}$) are selected to have a single, isolated electron or muon candidate with $E_T > 20 \text{ GeV}$, large imbalance in transverse momentum in the event ($\cancel{E}_T > 20 \text{ GeV}$) as expected from the undetectable neutrino, and at least four jets with $E_T > 20 \text{ GeV}$. Jets are reconstructed using a cone algorithm with radius $\Delta R = 0.4$ in $\eta - \phi$ space, and their energies are corrected for non-uniformities in the calorimeter response as a function of jet η , multiple $p\bar{p}$ interactions, and the hadronic jet energy scale of the calorimeter [18]. Of these jets, we require at least one to have originated from a b quark by using an algorithm that identifies a long-lived b hadron through the presence of a displaced vertex (b tag) [19]. Backgrounds to the $t\bar{t}$ signal arise from multi-jet QCD production (QCD), W -boson production in association with jets (W +jets), and electroweak backgrounds (EWK) composed of diboson (WW , WZ , ZZ) and single top-quark production. The W +jets background includes b -flavor jets (W +hf) as well as light flavor jets incorrectly identified as b jets (W +lf).

A detailed description of the background estimation can be found in Ref. [20]. Table I shows the expected sample composition assuming a $t\bar{t}$ cross section of 6.7 pb . There are overlapping events between those collected by high- p_T lepton triggers and \cancel{E}_T +jets trigger. These overlapping events are accounted in the central e/μ and forward e categories, and are explicitly vetoed from \cancel{E}_T +jets category.

TABLE I: Number of expected and observed events in 2.7 fb^{-1} assuming a $t\bar{t}$ cross section of 6.7 pb .

Process	Central	Forward	\cancel{E}_T +jets
	e, μ	e	μ
$t\bar{t}$	478 ± 66	58 ± 8	134 ± 19
W +hf	71 ± 22	13 ± 9	19 ± 6
W +lf	23 ± 6	5 ± 7	6 ± 2
EWK	17 ± 10	3 ± 1	5 ± 3
QCD	28 ± 22	46 ± 37	1 ± 1
Total expected	616 ± 74	125 ± 40	165 ± 20
Observed	650	136	178

The HERWIG [21] MC generator is used to model the $t\bar{t}$ signal events with $m_t = 175 \text{ GeV}/c^2$. For estimation of various systematic uncertainties and background modeling MC samples are created using the PYTHIA [22] generator, and ALPGEN [23] or MADEVENT [24] with PYTHIA or HERWIG supplying the parton shower and fragmentation. The QCD background is modeled using data control samples. The signal and background modeling has been extensively checked. Figure 1 compares the observed data and the MC-predicted distributions of different kinematic variables. We have validated the background model by studying a high-statistics control sample of W +jets candidates extracted by vetoing events containing b -tagged

jets.

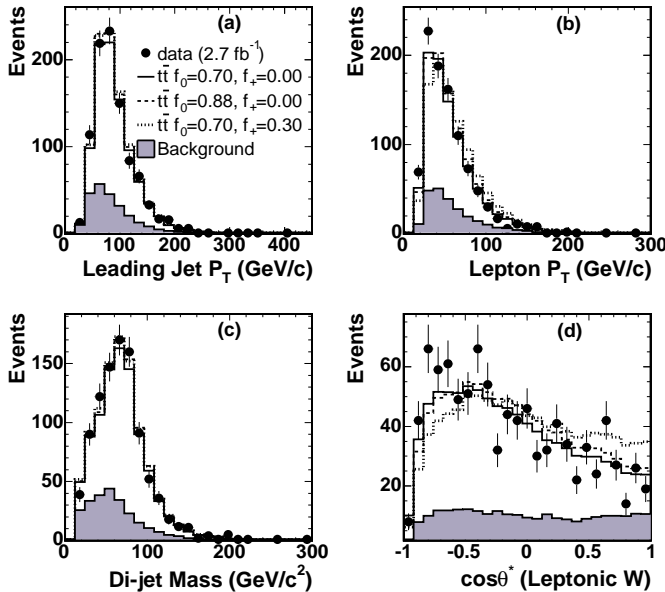


FIG. 1: Comparison of four kinematic variables for data and simulation for different W polarization fractions: solid, dashed and dotted histograms correspond to (f_0, f_+) values of $(0.7, 0.0)$, $(0.88, 0.0)$ and $(0.7, 0.3)$, respectively. Plotted are (a) leading jet p_T , (b) lepton p_T ; and for the reconstruction chosen as most likely by the per-event likelihood (c) the invariant mass of the pair of light quark jets from the hadronically decaying W boson and (d) the $\cos \theta^*$ of the leptonically decaying W boson.

We calibrate the results of the likelihood fit using the simulated $t\bar{t}$ and background samples, and the sample composition of table I. For the simultaneous measurement of f_0 and f_+ , we find our estimate $f_{0,m}$ is related to the true value of f_0 by $f_{0,m} = (0.88 \pm 0.02)f_0 + (-0.12 \pm 0.01)$ and our estimate of $f_{+,m}$ is related to the true value of f_+ and f_0 by $f_{+,m} = (1.26 \pm 0.01)f_+ + (0.17 \pm 0.02)f_0 + (0.06 \pm 0.01)$. We use these two equations and the measured polarization fractions to extract the true polarization fractions. For our measurement of f_0 with $f_+ = 0$, we find our estimate $f_{0,m} = (1.15 \pm 0.04)f_0 + (-0.09 \pm 0.02)$, and for our measurement of f_+ with $f_0 = 0.7$, we find our estimate $f_{+,m} = (1.17 \pm 0.05)f_+ + (0.01 \pm 0.01)$. The uncertainties on the coefficients of the calibration functions are accounted as the method-related systematic uncertainties, which cover possible biases due to the calibration procedure. The differences between $f_{0,m}$ or $f_{+,m}$ values and the corresponding true values are due to the fact that the signal and background probabilities in the the likelihood do not model events with extra jets from initial and final state radiation (ISR/FSR), or incorrect jet-parton assignment where a ISR/FSR jet is selected as one of the leading four jets, or all the different background pro-

cesses. Even though likelihood can be calculated only for the physical values of f_0 and f_+ , after calibration the corrected measured values can be slightly outside their physical ranges.

The robustness of the fitting procedure over all physical values of (f_0, f_+) has been tested with simulated experiments, using the number of observed data events and the sample composition of table I. In all cases, the fit is unbiased. Near the physical boundaries, we find that the statistical uncertainty is underestimated by as much as a factor of 1.5. We apply a correction to the statistical uncertainty in these regions. Assuming the SM, the expected statistical uncertainties after all corrections for the simultaneous measurement are ± 0.116 and ± 0.074 for f_0 and f_+ , respectively.

Various sources of systematic uncertainty affecting the measurement are summarized in table II. The leading sources of systematic uncertainty arise from MC modeling of initial and final state radiation (ISR/FSR), choice of parton distribution functions (PDFs), choice of parton shower model, uncertainties on the measured jet energy, and the background shape and normalization. The method-related uncertainty includes propagating the uncertainty on the fit parameters of the response curves, including their correlations. All systematic uncertainties are determined by performing simulated experiments in which the systematic parameter in question is varied, the default method and calibrations are applied, and the shifts in the mean measured polarization fractions are used to quantify the uncertainty. All shifts are evaluated at the SM helicity fraction.

TABLE II: Summary of systematic uncertainties.

Source	Δf_0	Δf_+	Δf_0	Δf_+
			simultaneous	
ISR/FSR	0.020	0.018	0.020	0.021
PDF	0.024	0.013	0.009	0.016
JES	0.018	0.017	0.004	0.012
Parton shower	0.012	0.008	0.031	0.017
Background	0.009	0.038	0.042	0.039
Method-related	0.010	0.005	0.024	0.024
b-tag SF	0.004	0.002	0.002	0.002
Total	0.041	0.048	0.062	0.057

For the simultaneous measurement of f_0 and f_+ , we exclude the events from the forward electron trigger as this significantly reduces the systematic uncertainty from the background model. With 828 events and after all corrections, we measure

$$f_0 = 0.879 \pm 0.106(\text{stat}) \pm 0.062(\text{syst})$$

$$f_+ = -0.151 \pm 0.067(\text{stat}) \pm 0.057(\text{syst}).$$

The statistical correlation between f_0 and f_+ is $\rho = -0.59$. We estimate a shift of $\mp(0.010 \pm 0.005)$ in f_0 and $\pm(0.017 \pm 0.003)$ in f_+ per $\pm 1 \text{ GeV}/c^2$ shift in the top quark mass from the central value of $175 \text{ GeV}/c^2$. As the central value is unphysical we have elected to ensure coverage by applying the Feldman-Cousins method [25] to obtain the confidence level (C.L.) intervals shown in Figure 2.

Fixing $f_+ = 0$ and with 964 events, we measure after all corrections $f_0 = 0.701 \pm 0.069(\text{stat}) \pm 0.041(\text{syst})$. Fixing $f_0 = 0.70$, we measure after all corrections $f_+ = -0.010 \pm 0.019(\text{stat}) \pm 0.049(\text{syst})$ and find $f_+ < 0.12$ at 95% C.L.. We estimate a shift of $\pm(0.011 \pm 0.003)$ in f_0 and $\pm(0.013 \pm 0.002)$ in f_+ per $\pm 1 \text{ GeV}/c^2$ shift in the top-quark mass from the central value of $175 \text{ GeV}/c^2$.

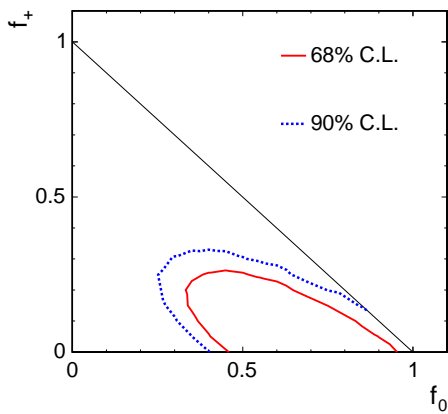


FIG. 2: Contours in the (f_0, f_+) plane indicating 68% and 90% C.L. intervals determined using Feldman-Cousins method. Note that the coverage is correct although the center of the contours is not at the measured value obtained after calibration.

In summary, we have measured the polarization of the W boson in top-quark decays using a matrix-element method in 2.7 fb^{-1} of CDF II data. Our results are consistent with the SM. This result improves the combined statistical and systematic precision on both the model-independent and model-dependent determinations of the longitudinal polarization f_0 by a factor of 1.3 compared to the best previous measurement [9] for a 1.4 times increase in luminosity.

We thank the Fermilab staff and the technical staffs of the participating institutions for their vital contributions. This work was supported by the U.S. Department of Energy and National Science Foundation; the Italian Istituto Nazionale di Fisica Nucleare; the Ministry of Education, Culture, Sports, Science and Technology of Japan; the Natural Sciences and Engineering Research Council of Canada; the National Science Council of the Republic of China; the Swiss National Science Foundation; the A.P. Sloan Foundation; the Bundesministerium für Bildung und Forschung, Germany; the World Class University Program, the National Research Foundation of Korea; the Science and Technology Facilities Council and the Royal Society, UK; the Institut National de Physique Nucleaire et Physique des Particules/CNRS; the Russian Foundation for Basic Research; the Ministerio de Ciencia e Innovación, and Programa Consolider-Ingenio 2010, Spain; the Slovak R&D Agency; and the Academy of Finland.

-
- [1] F. Abe *et al.* (CDF Collaboration), Phys. Rev. Lett. **74**, 2626 (1995); S. Abachi *et al.* (D0 Collaboration), Phys. Rev. Lett. **74**, 2632 (1995).
 - [2] Charge-conjugate modes are included implicitly throughout this paper.
 - [3] C. Amsler *et al.* (Particle Data Group), Phys Lett. **B667**, 1 (2008) and 2009 partial update for the 2010 edition.
 - [4] J. Aguilar-Saavedra *et al.*, Eur. Phys. J. C **50**, 519 (2007).
 - [5] T. Aaltonen *et al.* (CDF Collaboration), Phys. Rev. Lett. **99**, 151801 (2007).
 - [6] M. Fischer *et al.*, Phys. Rev. D **63**, 031501(R) (2001); H. S. Do *et al.*, Phys. Rev. D **67**, 091501(R) (2003).
 - [7] V. M. Abazov *et al.* (D0 Collaboration), Phys. Rev. Lett. **102**, 092002 (2009).
 - [8] V. M. Abazov *et al.* (D0 Collaboration), Nature **429**, 02589 (2004); V. M. Abazov *et al.* (D0 Collaboration), Phys. Lett. **B617**, 1 (2005).
 - [9] T. Aaltonen *et al.* (CDF Collaboration), Phys. Lett. **B674**, 160 (2009).
 - [10] A. Abulencia *et al.* (CDF Collaboration), Phys. Rev. Lett. **98**, 072001 (2007); A. Abulencia *et al.* (CDF Collaboration), Phys. Rev. D **75**, 052001 (2007); A. Abulencia *et al.* (CDF Collaboration), Phys. Rev. D **73**, 111103 (2006); D. Acosta *et al.* (CDF Collaboration), Phys. Rev. D **71**, 031101 (2005).
 - [11] We use a cylindrical coordinate system where the z axis is along the proton beam direction and θ is the polar angle. Pseudorapidity is $\eta = -\ln \tan(\theta/2)$, while transverse momentum is $p_T = |p| \sin \theta$, and transverse energy is $E_T = E \sin \theta$. Missing transverse energy, \cancel{E}_T , is defined as the magnitude of $-\sum_i E_T^i \hat{n}_i$, where \hat{n}_i is the unit vector in the azimuthal plane that points from the beam line to the i^{th} calorimeter tower.
 - [12] V. M. Abazov *et al.* (D0 Collaboration), Phys. Rev. Lett. **100**, 062004 (2008).
 - [13] A. Abulencia *et al.* (CDF Collaboration), Phys. Rev. Lett. **99**, 182002 (2007).
 - [14] G. Mahlon and S. Parke, Phys. Lett. **B411**, 173 (1997);

- G. Mahlon and S. Parke, Phys. Rev. D **53**, 4886 (1996).
- [15] F. A. Berends, W. T. Giele, and H. Kuijf, Nucl. Phys. B **321**, 39 (1989).
- [16] D. Acosta *et al.* (CDF Collaboration), Phys. Rev. D **71**, 031101(R) (2005).
- [17] A. Abulencia *et al.* (CDF Collaboration), Phys. Rev. D **74**, 072006 (2006); T. Aaltonen *et al.* (CDF Collaboration), Phys. Rev. Lett. **100**, 211801 (2008).
- [18] A. Bhatti *et al.*, Nucl. Instrum. Methods A **566**, 2 (2006).
- [19] D. Acosta *et al.* (CDF Collaboration), Phys. Rev. D **71**, 052003 (2005).
- [20] D. Acosta *et al.* (CDF Collaboration), Phys. Rev. Lett. **97**, 082004 (2006).
- [21] G. Corcella *et al.*, J. High Energy Phys. **01**, 10 (2001).
- [22] T. Sjostrand *et al.*, Comput. Phys. Commun. **135**, 238 (2001).
- [23] M. Mangano *et al.*, J. High Energy Phys. **07**, 001 (2003).
- [24] J. Alwall *et al.*, J. High Energy Phys. **09**, 28 (2007).
- [25] G. J. Feldman and R. D. Cousins, Phys. Rev. D **57**, 3873 (1998).